Designing timber connections for ductility – A review and discussion

(article starts on next page)

Designing timber connections for ductility – A review and discussion

Lisa-Mareike Ottenhaus [a,*], Robert Jockwer [b], David van Drimmelen [a], Keith Crews [a]

[a] *The University of Queensland, St Lucia QLD 4072, Australia*
[b] *Chalmers University of Technology, SE-412 96 Gothenburg, Sweden*

ABSTRACT

This paper discusses the design principles of timber connections for ductility with focus on laterally-loaded dowel-type fasteners. Timber connections are critical components of timber structures: not only do they join members, but they also affect load capacity, stiffness, and ductility of the overall system. Moreover, due to the brittle failure behaviour of timber when loaded in tension or shear, they are often the only source of ductility and energy dissipation in the structure in case of overloading, much like a fuse in an electrical circuit.

This paper addresses current challenges in connection design for ductility, reviews selected best-practice design approaches to ensure ductility in timber connections, suggests simple performance-based design criteria to design connections for ductility, and aims to stimulate a discussion around potential solutions to implement safe design principles for ductile connections in future design codes and connection testing regimes.

1. Introduction

McLain [1] stated that "a structure is a constructed assembly of joints separated by members" and this couldn't be truer for timber structures, where connections majorly influence the overall structural performance. Connections are often intended to act as potential ductile elements (PDEs), contributing significantly to overall ductility and energy dissipation in case of overloading [2] and allowing for safe load paths when construction tolerances are exceeded. PDE connections hence need to be designed as "fuses" to prevent brittle failure causing progressive and catastrophic collapse [3].

Examples of such discrete "fuses" are CLT shear wall hold-downs, beam-column joints in post-and-beam or post-and-plate systems, or column-base joints in portal frames, as well as more advanced connection systems including post-tensioning with dissipators or slip-friction joints [4–6]. Traditional light timber framing in low- to mid-rise construction does not rely on discrete fuses for ductility but instead activates an abundance of plastic deformation (often combined with a high degree of redundancy); e.g. in the nails connecting plywood sheathing to timber studs [7].

However, the focus on ductility under exceptional load alone is not enough, since connection behaviour also influences overall structural performance in terms of stiffness and capacity in the serviceability and ultimate limit state of members and sub-assemblies. Unsurprisingly,

connections were involved in 25% of cases in a study of almost 800 failures, damages and collapses [8–10]. Moreover, connections are the most complex and expensive elements in timber structures, both in terms of time required in design and production, as well as production resources and material cost.

1.1. Design criteria for potential ductile element connections

Accordingly, there are several design criteria for PDE connections which need to be met to provide adequate overall performance under both serviceability limit state (SLS) and ultimate limit state (ULS) load scenarios, including gravity, wind, snow, seismic, and live load from occupancy/traffic, as well as their load combinations.

It should be noted that this paper uses a Eurocode-style notation, but the concepts are applicable to any framework and design code that uses partial safety factors and is based on limit state design. Furthermore, the paper generally refers to forces "F" and displacements "Δ" for sake of simplicity but all concepts are equally applicable to moments "M" and rotations "θ".

1) As the name suggests, PDE connections need to be ductile, where ductility μ is defined as the ability to sustain load under increasing displacement. Ductility is extremely important as it gives sufficient warning through noticeable deformations before catastrophic brittle failure occurs [11]. A ductile connection response is often associated

Nomenclature

a_1	Fastener spacing parallel to the grain
a_2	Fastener spacing perpendicular to the grain
a_3	End distance
b_{net}	Net width of area that fails in block shear
d	Fastener or hole diameter
Δ	Displacement
Δ_{el}	Elastic displacement
Δ_{Fmax}	Peak displacement
Δ_{Fu}	Ultimate displacement
Δ_{Fy}	Yield displacement
Δ_{pl}	Plastic displacement
Δ_T	Target displacement
$E_{0,mean}$	Mean Young's modulus parallel to the grain
F	Force
F_b	Bottom shear plane capacity
F_{BR}	Brittle capacity
$F_{BR,conn}$	Brittle connection capacity
$F_{BR,mem}$	Brittle member capacity
$F_{BR,red}$	Reduced brittle capacity
F_{DUC}	Ductile load capacity
$F_{DUC,95\%}$	95th-percentile ductile capacity
F_{EYM}	European yield model capacity
F_{GT}	Group tear-out capacity
$F_{GT,red}$	Reduced group tear-out capacity
F_{max}	Peak load capacity
F_{NT}	Net tension capacity
F_p	Proportional limit capacity
F_{pre}	Connection pre-load
F_{PS}	Plug shear capacity
F_{RS}	Row shear capacity
$F_{RS,red}$	Reduced row shear capacity
$F_{s,l}$	Side shear plane

F_{SP}	Splitting capacity
F_t	Head tensile capacity
F_u	Ultimate load capacity
F_y	Yield load capacity
f_h	Embedment strength
$f_{h,e}$	Effective embedment strength at yield point
f_s	Shear strength
f_t	Tensile strength
f_u	Fastener ultimate tensile strength
f_y	Fastener yield tensile strength
G_{mean}	Mean shear modulus
γ_M	Partial material safety factor
γ_{Rd}	Connection overstrength
K	Foundation modulus
K_e	Elastic re-load stiffness
K_{el}	Elastic stiffness
K_s	Shear plane stiffness
K_{SLS}	Linear elastic stiffness
K_t	Head plane stiffness
L_s	Shear plane
$L_{s,red}$	Reduced shear plane
M	Moment
M_{ef}	Effective yield moment
M_{el}	Yield moment
M_{pl}	Plastic moment
μ	Ductility
n_1	Number of fasteners in a row parallel to the grain
n_2	Number of rows of fasteners
n_{ef}	Effective number of fasteners
t	Member thickness
t_{ef}	Effective thickness
θ	Rotation
θ_T	Target rotation

with plastic fastener deformation which allows for energy dissipation under reverse-cyclic loading, which is crucial for seismic design; Jorissen and Fragiacomo [11]) refer to this as "dynamic ductility". Furthermore, plastic deformations allow for load redistribution and activation of the load-carrying capacity of all fasteners in case of overloading, which is vital for structural robustness [11,12]. Finally, ductility is also of benefit in statically indeterminate systems where load redistribution leads to higher utilisation of the structural system [13].

2) PDE connections need to be designed to minimise slip and provide adequate stiffness K_{el} in the elastic region. This is especially important for tall timber buildings which are usually governed by the wind serviceability limit state, wherein connections with too little elastic stiffness compromise the overall lateral load system design [14]. More importantly, regardless of building height, excessive elastic deformations can lead to unintended load paths, and may even trigger violation of a stability limit state. The difference between K_{SLS} and K_e in the current Eurocode 5 draft should be noted, where the former can be derived from the load–displacement envelope curve in the linear elastic region and the latter is determined in the elastic re-loading cycles. In this paper, K_{el} is used as a placeholder for either K_{SLS} or K_e, depending on the load scenario and limit state.

3) PDE connections need to have "adequate" load capacity F_{DUC}, meeting demand without excessive amounts of connection over-strength [15] and this will be discussed further in the context of capacity design below.

4) Capacity design is required for seismic design because it ensures that mechanical connections which are detailed for low-cycle fatigue and

ductility — both of which are required for energy dissipation [16–18] — govern the response. However, it is applicable to all PDE connections, since the capacity hierarchy must be maintained to guarantee the intended structural response. Regardless of the load case, the PDE connection needs to be the weakest link in the capacity chain so that it can develop its intended ductility without premature brittle failure [2]. This is of particular importance for more complex and high-performance structures and in terms of robustness [12].

5) Finally, PDE connections need to dissipate energy and limit accelerations during high lateral load events such as windstorms and earthquakes, while simultaneously staying within acceptable limits of deformation and resulting overall structural and non-structural damage when the ultimate limit state design point is reached or even exceeded. The level of "acceptable" damage will depend on the load event and limit state, as well as intended post-disaster function of the structure [19]. It should be noted that for those structures with significant post-disaster function (e.g. bridges, hospitals, government buildings), a PDE connection detail with a self-centring mechanism (such as post-tensioning with accompanying dissipators or slip-friction joints) may be more appropriate, as it leads to lower residual deformations after overloading when compared to most dowel-type connections [6,20,21].

While many of the above aspects of PDE connection requirements are generally agreed upon in the research community, there is lively discussion around how to translate the requirements into design principles, and how to reflect and implement these in design codes. Moreover, considerable confusion exists in both education and practice disciplines

around interpretation of design codes, partly due to a range of unclear or contradicting definitions [8].

This paper aims to address some of these challenges, provide some clarifications where deemed necessary, highlight a selection of state-of-the-art best practice approaches, point out important areas of further research, and stimulate and contribute to academic discussion around potential solutions to implement safe design principles for ductile connections in design codes and connection testing regimes.

2. Discussion of design principles

2.1. How to write design codes – Discussion

In the past, design codes were often written as prescriptive rules to direct practitioners towards adopting a certain connection layout without explaining the underlying reasons for certain design choices, configurations, load and deformation limits, or material choices [22]. While some see this approach as patronising, ultimately, its intention has been to facilitate safe design through prescriptive best practice and implicit safeguards. Common examples of prescriptive safeguards are minimum fastener spacings and edge distances, slenderness ratios of fasteners (assuring plastic hinging), minimum number of fasteners (i.e. 2 for redundancy), the effective yield moment M_{ef} in Eurocode 5 which favours smaller diameter fasteners, assuming that full plasticity cannot be achieved in large diameter fasteners [23], or the effective number of fasteners n_{ef} which is intended to prevent inadequate fastener spacing or using too many fasteners in a row causing unequal force distribution, both of which may ultimately result in brittle failure [24].

It could be argued that design codes should not introduce an excessive amount of complexity and should not require in-depth understanding of advanced theory, such as fracture mechanics or non-linear analysis. Instead, they should offer simple design guidelines based on best practice, which reduces time spent on the design task and reduces cost, while offering sufficient freedom to make more innovative design choices.

Many current structural designs in low- and mid-rise construction already rely on standardised and simplified approaches, spreadsheets, and software design tools. Simple design guidance also makes the design of advanced and modern timber structures more accessible, which is desperately needed for design professionals in order to reduce the entrance barrier towards timber structures, assure their safety, prevent unnecessary errors, and ultimately make timber structures more competitive with other structural building materials.

More importantly, complex models are more prone to user errors especially if there is a lack of understanding of the underlying theory, which increases the risk of misinterpretation or unbeneficial design choices. Hence, rather than introducing unfounded calibration factors and "safeguards", it is important to guide and explain why certain designs may perform better than others, facilitating understanding among practitioners.

However, there is a fine line between simple models and oversimplification that becomes inefficient, hinders innovation, and may be even unsafe due to misinterpretation [25,26]. Despite warnings and specification of limitations, simplified models are often used outside of their context and intended scope. One such example is the connection strength tables in the Australian timber structures standard, AS 1720.1 [27], the derivation of which is not transparent and is often poorly understood since practitioners may lack knowledge of connection design theory. Attempts have since been made to combine these strength tables with the European Yield Model (EYM) [19,28].

Therefore, design codes need to strike a balance between simplicity for standard scenarios, whilst providing more accurate and advanced design methods that enable experts to design more complex and advanced connections safely [25,26].

Hence, it is recommended to split connection design chapters into different parts: 1) simplified parts with very clear limitations but high levels of ease of application, and 2) other parts (or annexes) that provide detailed and more sophisticated rules. The simplified parts still need to convey the minimum required understanding of the underlying theory, ideally to a small extent in the design code itself, and both parts should be accompanied by detailed commentary which contains best practice worked examples and references to relevant publications, as well as details of the assumptions made by the code committee members during development of the code itself. The split between simplified rules and more detailed and sophisticated design approaches is currently applied in the Swiss standard for timber structures SIA 265 [29].

2.2. Connection overstrength and capacity design

Capacity design ensures that PDEs can develop their intended ductility by protecting all brittle failure mechanisms from PDE connection overstrength. This creates a capacity hierarchy where the ductile response becomes the "weakest link" [2,15,30].

Connection overstrength γ_{Rd} is defined as the ratio between the calculated ductile design capacity in design codes $F_{DUC,d}$ and the capacity the connection may develop in reality under ductile response. Connection overstrength might stem from intended or unintended conservatism in the design equations, variations in the material strength (actual higher strength than that considered in design), or from second order effects (rope effect, friction, etc.) in the connection [11,31]. Since actual ductile connection capacity is hard to quantify, connection overstrength is often derived using the 95th-percentile in the ductile capacity distribution $F_{DUC,95\%}$ as shown in Eq. (1), either through experimental testing or by using analytical models [31,32]

$$\gamma_{Rd} = F_{DUC,95\%}/F_{DUC,d} \text{ with } F_{DUC,d} = min\{F_{EYM,i,d}\}; i = 1...n \tag{1}$$

where i designates the EYM mode and there are n modes for a given connection layout. It should be noted that both ductility and energy dissipation through repeated plastic deformation of metal fasteners need to be guaranteed under seismic loading; hence, EYM modes that rely on embedment alone should be avoided [25,26].

To achieve the intended ductility, all brittle failure modes (both within the connection and members) need to be capacity protected; i.e. the brittle design capacity $F_{BR,d}$ needs to exceed the actual connection capacity, which is defined as the ductile design capacity multiplied by its overstrength $F_{DUC,d} \gamma_{Rd}$, where $F_{DUC,d}$ is the peak capacity of the connection $F_{max,d}$ developed under ductile response. The capacity hierarchy can be expressed as $F_{BR,d} \geq \gamma_{Rd} F_{DUC,d}$.

The brittle design capacity is given in Eq. (2):

$$\begin{aligned} F_{BR,d} &= min\{F_{BR,conn,d}, F_{BR,mem,d}\} \\ \text{with } F_{BR,mem,d} &= min\{F_{BR,mem,j,d}\}; j = 1...m \\ \text{and } F_{BR,conn,d} &= min\{F_{RS,d}, F_{GT,d}, F_{SP,d}, F_{PS,d}, F_{NT,d}\} \end{aligned} \tag{2}$$

where $F_{BR,mem,d}$ is the governing brittle member design capacity, j designates the type of brittle member failure and there are m brittle failure modes for a given member; e.g. tensile rupture, shear, bending. $F_{BR,conn,d}$ is the governing brittle connection design capacity, with row shear capacity F_{RS}, group tear-our capacity F_{GT}, splitting capacity F_{SP}, plug-shear capacity F_{PS}, and net tensile capacity F_{NT}. Note that a subset of capacities applies to a specific connection type; for example, splitting usually occurs for connections with one row of fasteners, whilst plug-shear can only occur in a connection with nails, screws or rivets that only partially penetrate the timber member. It is also important to note that brittle and ductile design capacities are obtained by dividing the respective characteristic capacity by its partial material safety factor γ_M (which depends on the distribution characteristics of the type of timber material and anticipated failure mode and is specified accordingly), as well as multiplication by force modification factors that account for load duration, temperature, moisture content, etc. (and this will be specific to the particular design code).

2.3. Ductility and yield point – Discussion

Stehn and Björnfot [33] presented 12 different ductility definitions and there has been much discussion around which one of these is most appropriate to use for timber connections. While researchers can examine a load–displacement curve and intuitively judge whether the behaviour is brittle or ductile, the research community continuously struggles to arrive at a universally accepted definition that works without occasionally misclassifying a ductile connection as brittle and vice versa; and some of these shortcomings will be explicitly highlighted below.

Without going into a detailed discussion regarding the yield point, Fig. 1 gives an example of a ductile load–displacement curve as a reference, with elastic stiffness K_e, yield capacity F_y and yield displacement Δ_{Fy}, peak capacity F_{max} and respective displacement Δ_{Fmax}, and ultimate capacity F_u at point of failure (or $F_u = 0.8\,F_{max}$, whichever occurs first) with ultimate displacement Δ_{Fu}. Eq. (3.1) to Eq. (3.12) give the 12 ductility definitions, which were adapted from Jorissen and Fragiacomo [11], and these will be evaluated against suitability criteria below.

$$\mu = \Delta_{Fmax}/\Delta_{Fy} \tag{3.1}$$

$$\mu = \Delta_{Fu}/\Delta_{Fy} \tag{3.2}$$

$$\mu = \Delta_{Fu}/\Delta_{Fmax} \tag{3.3}$$

$$\mu = \left(\Delta_{Fmax} - \Delta_{Fy}\right)/\Delta_{Fmax} \tag{3.4}$$

$$\mu = \left(\Delta_{Fu} - \Delta_{Fy}\right)/\Delta_{Fu} \tag{3.5}$$

$$\mu = K_e/F_1\Delta_{Fmax} \text{ where } F_1 = max\,F(0 \leq \Delta \leq 5\text{mm}) \tag{3.6}$$

$$\mu = K_e/F_1\Delta_{Fu} \text{ where } F_1 = max\,F(0 \leq \Delta \leq 5\text{mm}) \tag{3.7}$$

$$\mu = \Delta_{Fmax} - \Delta_{Fy}[mm] \tag{3.8}$$

$$\mu = \Delta_{Fu} - \Delta_{Fy}[mm] \tag{3.9}$$

$$\mu = \Delta_{Fu} - \Delta_{Fmax}[mm] \tag{3.10}$$

$$\mu =_{\Delta=0}\int^{\Delta=\Delta Fmax} f(F,\Delta)d\Delta[Nmm] \tag{3.11}$$

$$\mu =_{\Delta=0}\int^{\Delta=\Delta Fu} f(F,\Delta)d\Delta[Nmm] \tag{3.12}$$

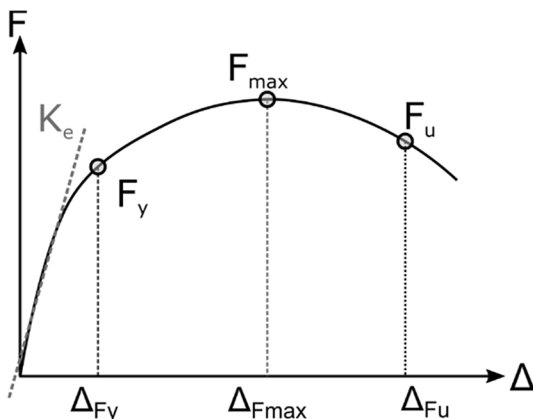The ductility definitions in Eq. (3.1) to Eq. (3.12) can be grouped into absolute and relative criteria, that are either based on deformations at maximum or at ultimate load. The different definitions raise the problem of defining ductility levels to distinguish ductile from brittle behaviour. Depending on the shape of the load-deformation curve, the different definitions may lead to considerably different ductility levels for the same curve.

Many researchers have recognised the issue of ductility misclassification and suggested new definitions to alleviate the problem. E.g. Flatscher [34] suggested a new definition that uses an equivalent plastic displacement and a shape parameter to avoid misclassification. Nevertheless, this definition still needs a scaling factor to be applicable to high capacity connections [35].

In the context of this paper, ductility is defined as *the ability to sustain a given load under increasing displacements*, which is a widely accepted ductility definition.

If this definition is used as the basis of connection design, then any discussions around which of the 12 different ductility definitions to use becomes almost superfluous: an absolute definition is more suited than a ratio and this has been previously pointed out by Jorissen and Fragiacomo [11].

Nevertheless, it is worth revisiting the ductility definitions and assessing their validity against some simple criteria to determine the most suited definition:

1) If a certain target displacement can only be achieved with excessive strength loss, the connection is not ductile. Any ductility definition that falsely classifies such a connection as ductile, is not applicable.

Using this criterion, definitions that rely on energy alone, such as Eq. (3.11) and Eq. (3.12), are invalid. The problem is illustrated in Fig. 2: both curves enclose the same area and therefore result in the same energy at $F_u = F_{max}$. However, while not particularly strong, only the lower of the two can be classified as ductile since the other displays perfectly brittle behaviour.

In addition, calculating the area under the load–displacement curve is impractical for hand calculations. Hence:

2) If the definition requires the calculation of energy, it is deemed impractical and not applicable.
3) Post-peak behaviour is essential to classify ductility as illustrated in Fig. 3: if only F_{max} is considered, both curves achieve the same ductility. However, most engineers would agree that softening behaviour is important, i.e. strength loss at increasing post-peak displacement should be gradual.

Hence, if the definition doesn't take post-peak behaviour into account, it does not capture the entire displacement-ability or "fuse action"
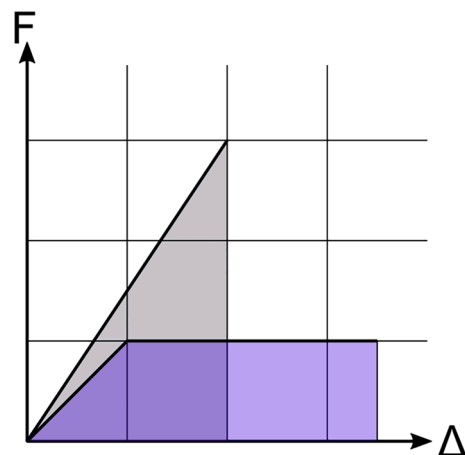

Fig. 1. Exemplar ductile load–displacement curve.

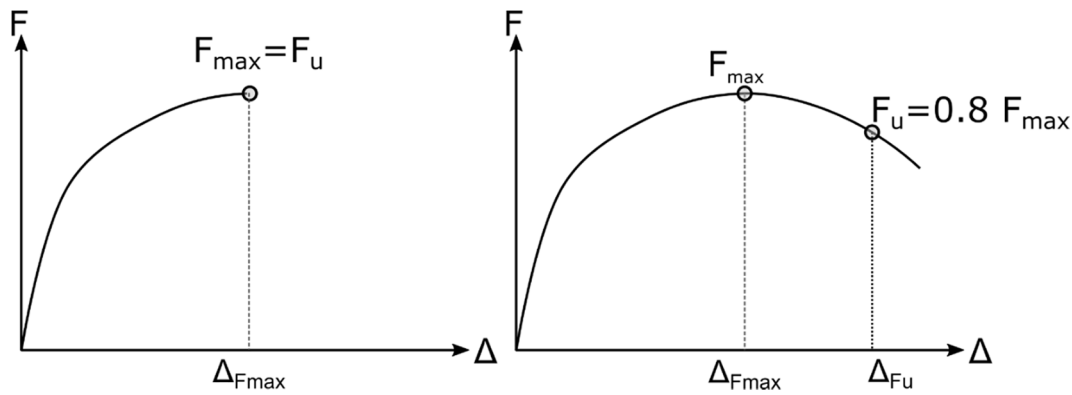**Fig. 2.** Energy defined by load–displacement curves.

Fig. 3. Examples of two load–displacement curves without and with softening.

and is not appropriate – this removes definitions given in Eq. (3.1), Eq. (3.4), Eq. (3.6), and Eq. (3.8) if used alone. Moreover, definitions given in Eq. (3.3) and Eq. (3.10) only capture softening and aren't applicable if used only by themselves.

4) If the definition produces vastly different ductilities for variations in initial stiffness while the load–displacement curves look very similar and achieve the same final displacement, it is not applicable.

In Fig. 4, both the dashed and solid curve have a very similar shape, and obtain the same yield strength F_y, peak strength F_{max}, and ultimate strength F_u. The only difference is the elastic / initial stiffness K_e, with $K_{e1} \approx 2 K_{e2}$. Since the initial stiffness is known to vary quite significantly even within one series of connection experiments, such a large difference is not extraordinary [36].

As an example, assume $\Delta_{Fy1} = 0.2$ mm and $\Delta_{Fy1} = 0.5$ mm, with $\Delta_{Fmax} = 1.5$ mm and $\Delta_{Fu} = 2.3$ mm. Using a definition that uses a ductility ratio such as definition Eq. (3.1), the solid line gives a relative ductility of $\mu_1 = 3$, whereas the dashed line gives a ductility of $\mu_2 = 7.5$. According to a classification system such as Smith et al. [37], the solid curve would thus be low-ductile, whereas the dashed curve would be highly ductile. Clearly, neither connection is ductile if the final displacement is considered.

One might also argue that, in practice, the difference between the curves is likely irrelevant, since both Δ_{Fy1} and Δ_{Fy2} are often in the order of few millimetres or less – no more than inherent slip in most bolted connections.

Consequently, any definition that uses a relative ductility based on the yield point or the elastic stiffness, is inadequate, including
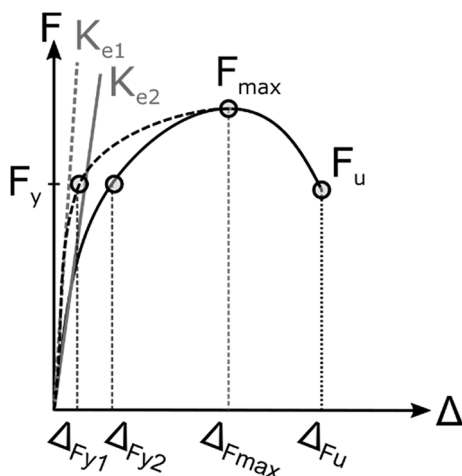
definitions given in Eq. (3.1), Eq. (3.2), Eq. (3.6), and Eq. (3.7).

While the above criteria have excluded some stand-alone ductility definitions, this does not imply that combinations of those definitions are invalid. On the contrary, combinations of those definitions may produce quite useful tools to classify ductility.

2.3.1. The yield point challenge

Most ductile timber connections do not yield at one single point but rather transition gradually from linear elastic to plastic behaviour while capacity often keeps increasing, as illustrated in Fig. 5. The "yielding" of the connection is owed to a combination of non-reversible timber crushing / fastener embedment and plastic yield deformation of the fastener. Upon load reversal, this plastic fastener deformation may reverse, whereas the timber embedment deformation generally remains and is irreversible.

At the yield point, the yield strength F_y and corresponding yield displacement Δ_{Fy} can be defined. It is generally agreed that the yield point is located somewhere between the proportional limit F_p (where the connection response is no longer linear elastic) and the peak strength F_{max}. However, since the transition from linear elasticity to plasticity is generally gradual, it is rather difficult to intuitively pin-point this yield point as shown in Fig. 5.

Muñoz et al. [38] listed six different methods to derive the yield point (not listed in the same order):

1) A method proposed by Karacabeyli and Ceccotti [39] for shear walls in light timber framed construction where the yield strength is taken as $F_y = 0.5 F_{max}$.
2) A method proposed by Yasumura and Kawai [40] and adopted by the Japanese HOWTEC [41] for light timber framed construction where a secant is fitted through 40% and 90% of F_{max}.
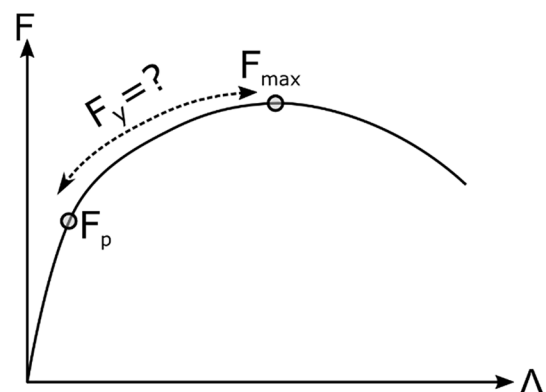

Fig. 4. Influence of stiffness on relative ductility definitions.

Fig. 5. Schematic representation of possible yield point location.

3) The Equivalent Energy Elastic–Plastic (EEEP) method suggested by Foliente [42] which approximates the elastic–plastic behaviour of an assembly.

4) The 5%-offset method which is used e.g. to determine the embedment yield load of dowels and bolts in ASTM D5764-97a [43], Smith et al. [37] suggested a similar offset method to determine system ductility, with an offset of 0.1 mm for translations, and 0.002 rad for rotations.

5) A method proposed by CSIRO which defines the yield displacement as 1.25 times the displacement at 0.4 F_{max}, $\Delta_{Fy} = 1.25\ \Delta_{0.4Fmax}$.

6) The $1/6^{th}$ method adopted by EN 12512 [44] and Swiss SIA Standard 265 [29] which defines test methods of the cyclic testing of joints with mechanical fasteners.

The first and second method are clearly designed for light timber framed construction and nailed assemblies rather than connections. In consequence, the method by Karacabeyli and Ceccotti [39] finds a yield point, even if the overall behaviour is essentially perfectly brittle.

Muñoz et al. [38] noted that the EEEP method often results in unrealistic values.

While simple, the 5%-offset method is not generally applicable: the appropriate offset depends on the number of fasteners, the diameter(s) of those fasteners, the connection geometry, and whether the assembly is loaded under tension or compression.

Depending on the extent of the linear elastic zone, the CSIRO method might produce yield points lower than the proportion limit.

The $1/6^{th}$ method is one of the most popular methods in conjunction with ductility definitions given in Eq. (3.1) and Eq. (3.2). However, the method is highly dependent on the initial stiffness and slight variations in yield displacement Δ_{Fy} can heavily skew the ductility ratio as previously shown and can produce misleadingly high ductilities even for brittle connections [35]. As a result, this definition becomes meaningless.

It should also be noted that the EEEP method, the $1/6^{th}$ method, and the method proposed by Yasumuara and Kawai [40] produce yield points that don't lie on the load–displacement curve and have little physical meaning. Finally, analysis of experimental data often requires some interpretation, such as a correction of slip, which introduces a level of subjectivity that is not captured by the testing standard.

For the purpose of (finite element) modelling it may be desirable to implement experimental results as parametrized data, that allow for a precise definition of the yield point. Proposals for parametric curves and corresponding data can be found for embedment behaviour of fasteners in Schweigler et al. [45] and for screw connections in Flatscher [34]. A database with a variety of test data is summarized in Schweigler et al. [46].

In order to choose an appropriate method to derive the yield point, several criteria should be met:

- The method should be simple, intuitive, and allow for simple hand-calculations in a laboratory setting; therefore, the calculation of energy or fitting of a tangent should be avoided.
- The method should reflect reality and be relevant to practice; ideally the yield point should lie on the experimental load–displacement curve.
- The method should not overestimate ductility.

2.3.2. Defining target displacement – A possible solution

In light of the issues related to the yield point definition, a better approach may thus be to avoid defining a specific yield point or yield displacement altogether as suggested by several researchers, including Flatscher [34].

Instead, different target displacements Δ_T can be defined that can be directly derived from an experimental load–displacement curve and are related to the role of the ductile connection in the overall structure:

- The **elastic displacement** of a connection's load–displacement curve can be determined by fitting a straight line to the elastic portion (e.g. between 10% and 40% F_{max}, although this may have to be evaluated on a case-by-case basis) and a significant sustained deviation off this line is then defined as the onset of yielding or proportional limit F_p with elastic deformation Δ_{el}.
  - Elastic deformations need to be limited to guarantee required initial stiffness and avoid unfavourable redistribution of load, non-structural damage, potential stability issues, etc.
  - The elastic limit will depend on the intended use of the connection; i.e. whether a connection is designed to be "soft" (low initial stiffness) or "rigid" (high initial stiffness).
- The **total plastic displacement** is defined as $\Delta_{pl} = \Delta_{Fu} - \Delta_{el}$.
- The authors suggest that, if the peak point is chosen as the design point, **post-peak behaviour** needs to be considered in the design, and should constitute at least 1/3 of the total plastic displacement to allow for sufficient ductility after overloading $\Delta_{Fu} - \Delta_{Fmax} \geq 1/3\ \Delta_{pl}$. The authors encourage discussion around what is an appropriate value for post-peak displacement.
- Total deformation requirements, or target displacement Δ_T can often directly be derived from target drifts and resulting rotation or uplift in a column base joint, shear wall hold-down, or beam-to-column joint; and this will be illustrated for a rocking shear wall below.
- Conservative assumptions regarding the system behaviour need to be made unless experimental data is available.

2.3.2.1. Example of shear wall hold-down design. To illustrate the derivation of the target displacement Δ_T and according selection of a suitable connection detail, consider a 1.5 m long shear wall with corner hold-downs and a central shear key connection as depicted in Fig. 6. The central shear key has vertically slotted holes to avoid uptake of hold-down forces[6] and is designed to remain elastic, through capacity design, while the corner hold-down connections are designed to yield during a ULS seismic event. As such, the wall is forced into a desirable rocking mechanism which will "self-centre" under the weight of the building after the seismic actions cease. Assuming that a stability limit of 2.5% governs the horizontal drift of the wall, and the shear and bending deformations make up 10% of the total horizontal drift, then the required ultimate displacement in a corner hold down is 90% of the rocking uplift associated with 2.5% horizontal drift: $\Delta_T = 0.9 \cdot 2.5\% \cdot 1.5$ m = 34 mm. Taking a displacement-based design approach, similar to Calvi et al. [47], an analysis could then determine the force on the shear wall by considering the energy dissipation and ductility of the building (or assembly) as a system. The assumption around shear and bending deformation can be verified or adjusted through iteration and the hold-downs can be detailed for the required displacement and force demand. It could be argued that the ultimate point (F_u, Δ_{Fu}) should be used to ensure collapse prevention at the maximum considered event, and the maximum point (F_{max}, Δ_{Fmax}) should be used to ensure life-safety at the ultimate limit state. While discussion around when and how to utilise target displacements is strongly encouraged, the remainder of the paper compares the ultimate displacement to the target displacement for consistency.

Assuming the force demand is below 150 kN, traditional (force-based) design would allow for selection of any nominally ductile connection that meets that demand and provides a reasonably stiff elastic response. Brown and Li [32] and Ottenhaus et al. [48] both investigated CLT hold-downs with 4 dowels and an internal steel plate in 5-layer CLT, with the difference being that Ottenhaus et al. used a "standard" spacing of 5d parallel to the load direction (both between fasteners and end distance) and 3d perpendicular to the load direction (d being the dowel diameter); while Brown and Li used a spacing of 5d parallel to the load direction, an end distance of 7d, and an increased row spacing of 6d perpendicular to the load direction.
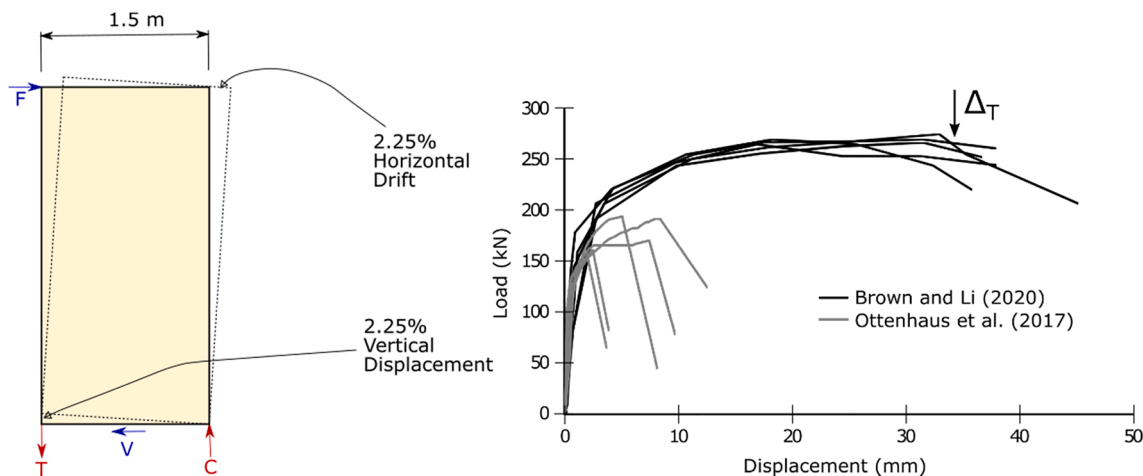
Fig. 6. Free-body diagram and rocking displacement of CLT shear wall example (left) and hold-down backbone load–displacement curves reproduced from Brown and Li (2020) and Ottenhaus et al. (2017) with target displacement Δ_T (right).

Brown and Li [32] found average ultimate deformations of $\Delta_{Fu} = 40$ mm and average $F_{max} = 270$ kN. The ductility ratio was $\mu = \Delta_{Fu} / \Delta_{Fy} = 18.5$.

Ottenhaus et al. (2017) achieved average values of $\Delta_{Fu} = 5.7$ mm, $F_{max} = 176$ kN and $\mu = \Delta_{Fu} / \Delta_{Fy} = 8.4$.

Arguably, only the modified hold-down connection by Brown and Li [32] meets the target displacement requirement Δ_T when displacement-based design is applied, while force-based design suggests that the connection investigated by Ottenhaus et al. [49] is a more economical solution, by meeting force demand and being nominally ductile (and therefore reducing force demand in force-based design).

The optimal design likely lies somewhere in the middle, with a capacity F_{max} that slightly exceeds the force demand and ultimate connection displacement-ability that is able to accommodate the target displacement ($\Delta_{Fu} \geq \Delta_T$). For many cases, the target displacement may be less than the stability criteria, which is used in the above example. For force-based design, the target displacement may be that which ensures the assumed system ductility is valid.

While this example identifies the importance of displacement performance in the context of seismic design, it is desirable to be able to predictably redistribute forces and dissipate energy under any form of reverse cyclic loading. For instance, design of critical connections which respond to wind loading should, arguably, still be able to accommodate some level of reversible plastic deflection, even if the system is designed elastically for the ULS wind event. Chuang and Spence [50,51] developed a performance-based model which accounts for the inelastic behaviour of structural systems subjected to probabilistic wind loading.

Finally, the authors acknowledge that the above approach is merely one method to define ductility criteria while avoiding the yield point challenge; as such, scientific discourse around this issue is strongly encouraged.

2.4. Design point for ductility – Discussion

Returning to the definition of ductility, a ductile connection needs to have the ability to sustain a given load under increasing displacements; however, it may be acceptable to allow for a certain decrease in the load level with increasing deformation without denoting it as failure.

Fig. 7 displays a ductile load–displacement curve with respective loads and displacements: elastic stiffness K_{el}, proportional limit capacity F_p with elastic displacement Δ_{el}, yield point (F_y, Δ_{Fy}), peak point (F_{max}, Δ_{Fmax}), and ultimate point (F_u, Δ_{Fu}). The plastic deformation is defined as $\Delta_{pl} = \Delta_{Fu} - \Delta_{el}$.

The load at failure, or ultimate load capacity F_u, is defined differently for static and cyclic loading: according to EN 26891 [52], for the
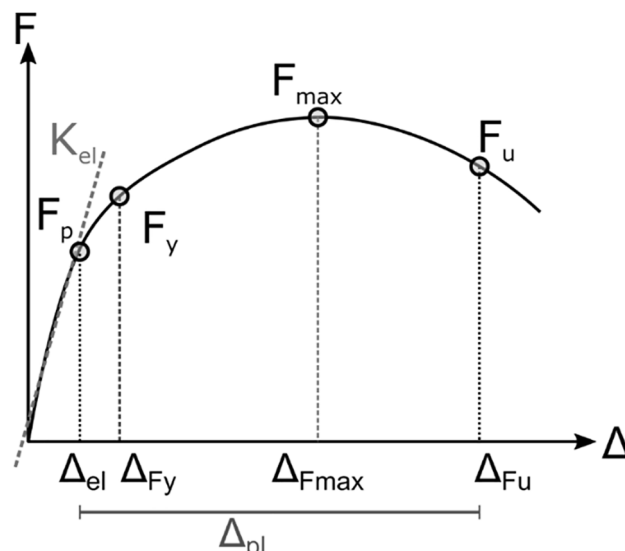

Fig. 7. Ductile load–displacement curve with elastic and plastic displacements.

determination of strength of joints made with mechanical fasteners under static conditions, the ultimate load capacity F_u is defined as the load reached before or at a slip of 15 mm. In EN 12512 [44], for the cyclic testing of joints made with mechanical fasteners, the ultimate load is defined at 80% of the maximum load ($F_u = 0.8 F_{max}$) or at a joint slip of 30 mm, whichever occurs first in the test. This approach is somewhat problematic, as even static overloading may lead to displacements $\Delta_T \geq 15$ mm.

While the designation "ultimate load" might insinuate that F_u corresponds to the design point for ultimate limit state, this is generally not the case. Instead, the maximum or peak capacity F_{max} is generally taken as the ULS design point which is also relevant for the capacity hierarchy in capacity design. While F_{max} is appropriate in terms of meeting capacity demand, the accompanying displacement Δ_{Fmax} does not reflect post-peak behaviour and cannot ensure ductility, while simultaneously exceeding acceptable displacement limits for low-damage design.

A better approach might be to define minimum performance criteria for PDE connections rather than a specific design point. These are independent of the type of loading (static, cyclic); however, seismic loading imposes additional requirements (energy dissipation, hysteresis that limits pinching), and these are covered in the literature [2,14].

The suggested performance criteria for PDE connections are then as

follows:

- An ultimate displacement Δ_{Fu} at $F_u = 80\%\ F_{max}$ that meets or exceeds the target displacement Δ_T (defined by structural response / required drift).
- A permissible elastic displacement Δ_{el} at the proportional limit F_p.
- A target yield capacity F_y where no significant plastic deformation has occurred $F_p \leq F_y \leq F_u$. This yield capacity can be calculated with the EYM using the fastener bending moment at onset of yielding $M_{el} = f_y\ \pi\ d^3\ /32$ and effective embedment strength $f_{h,e}$ as shown in Ottenhaus et al. [49,53] and this is further discussed below.
- F_y should be used as the target capacity for low-damage scenarios that are defined by performance criteria, such as SLS and some ULS cases; e.g. low-damage design of high-importance structures with post-disaster function, structures susceptible to low-cycle fatigue, and systems that require a strength reserve. Experimental studies on dowelled PDE connections in CLT by Ottenhaus et al. [54] and Brown and Li [32] suggest that F_y ranges between 70% and 80% of F_{max} for mild steel fasteners.
- F_{max} can be calculated using the EYM with the plastic moment $M_{pl} = f_y\ d^3\ /6$ and embedment strength f_h. F_{max} may be used as the target capacity for all other scenarios, predominantly related to life-safety. In those cases, post-peak behaviour of Δ_{Fu} - $\Delta_{Fmax} \geq 1/3\ \Delta_{pl}$ is desirable.
- Regardless of the target capacity, $F_{max,d} = F_{DUC,d}$ needs to be used to maintain the capacity hierarchy $F_{BR,d} \geq \gamma_{Rd}\ F_{max,d}$.

This approach achieves ductility and ensures safe design by providing both a capacity reserve for catastrophic overloading where this is mandated, and a displacement reserve to accommodate target displacements. The overall design philosophy is neither displacement-based nor force-based, but rather performance-based, where a target capacity exceeds demands, elastic deformations are limited, the capacity hierarchy is guaranteed, and permissible drift can be accommodated.

It should be noted, that in order for such an approach to be implemented, changes need to occur in the community of practice: 1) manufacturers need to start supplying yield strength values f_y for their fasteners, as well as displacement values such as Δ_{Fmax} and Δ_{Fu} for standard connection details in common timber materials; 2) experimental standards such as EN 26891 [52] and EN 12512 [44] need to be updated to mandate loading until 20% strength loss (or more) has occurred.

2.5. Ductile connection capacity – state-of-the-art

Using the EYM, both F_y and F_{max} can be predicted as illustrated by Ottenhaus et al. [49,53]. F_y is the minimum of all EYM equations using the effective embedment strength $f_{h,e}$ and elastic fastener moment (onset of yielding) $M_{el} = f_y\ \pi\ d^3/32$. F_{max} is the minimum of all EYM equations using the embedment strength f_h and plastic fastener moment (perfect plastic hinge) M_{pl}. It should be noted that fastener embedment alone (EYM mode Ia and Ib) does not provide connection ductility, as it leads to slip and pinching of hysteresis curves [14], which in turn leads to excessive displacements and unfavourable load paths [2]. Moreover, dowel-type connections that are subjected to reverse cycling loading or vibrations (such as windstorms, earthquakes, ocean waves, or traffic loading) need to be designed for reversible plastic fastener deformations.

2.5.1. Embedment strength – Discussion

Several parameters affect embedment strength, such as surface roughness of the fastener [55,56], fastener hardness [57], and initial contact area [58].

Furthermore, ongoing discussion around which experimental embedment test procedure to use continues to be unresolved, as there are currently three different standards to derive embedment strength

with half-hole or full-hole embedment testing: ASTM D 5764-97a [43], AS/NZS ISO 10984.2 [59], and EN 383 [60]. These have been discussed by Franke and Magnière [61], who recommended to derive embedment strength f_h from half-hole tests with the 5%-offset method and stiffness K (foundation modulus) from full-hole tests. While there is merit in conducting full-hole tests since these resemble actual steel-to-timber connections, it is important to choose a setup that reflects available cross sections: for mass timber panels (CLT, CLT-LVL, or Ply-Lam) as well as other engineered wood products such as Glulam and LVL, full-hole testing isn't possible (or relevant) since the embedment strength exceeds the dowel bending moment [35] unless the actual fasteners are replaced with very high strength steel for the purpose of full-hole embedment testing [62].

Apart from the research findings suggested by Yurrita and Cabrero [57], further experimental investigations are needed to reliably convert half-hole stiffness results into the corresponding full-hole stiffness. Moreover, embedment strength is severely affected by moisture content variations and future formulas should take this into account. Finally, Ottenhaus et al. [49,53] suggested that the elastic embedment strength may be approximated as $f_{h,e} \approx 0.8\ f_{h5\%}$ which is used to predict the yield capacity F_y. This assumption was based on 331 dowel embedment tests in New Zealand CLT [63] and needs to be verified for different fastener diameters, moisture contents, and timber materials.

2.5.2. Yield moment – Discussion

As outlined in Ottenhaus et al. [31], the effective yield moment $M_{ef} = 0.3\ d^{2.6}\ f_u$ assumes that full plasticisation of stocky fasteners is hardly achieved in timber connections [64]. However, Ottenhaus et al. [48] and Brown and Li [32] achieved perfect plastic hinges in dowelled connections with d = 20 mm and capacities ranging between 200 and 1500 kN.

Rather, the elastic section modulus should be used to predict F_y with $M_{el} = f_y\ \pi\ d^3\ /\ 32$ and the plastic fastener bending moment $M_{pl} = f_y\ d^3\ /\ 6$ to predict F_{max} [31,49].

An issue with this approach is that many fastener design codes only specify f_u and not f_y. Generally, fastener manufacturers only determine f_u in experimental testing since f_y can be very difficult to derive from experimental testing, especially for high strength steel as shown in Fig. 8. Hence, a conversion factor from f_u to f_y may be applied as suggested by Blass and Colling [65].

The yield moment can either be derived by conducting a tensile test on the fastener or by three point bending as outlined in AS/NZS ISO 10984.1 [66].

For pure tensile tests, either the yield plateau or the proportional limit can be taken as the yield load; the yield strength is then determined as $f_y = F_y\ /\ [\pi(d/2)^2]$.

For three-point bending, the yield point is defined by a slight change in stiffness. The elastic moment is $M_{el} = F_y\ L\ /\ 4$, where L designates the distance between the supports. The plastic moment can be calculated directly as $M_{pl} = 1.698\ M_e$.

The ultimate tensile strength f_u is relevant to prevent rupture of the fastener which can be critical for high strength steel where the $f_u\ /\ f_y$ ratio is low. For lower ductility connections that do not act as PDEs, high-strength steel may be employed which brings F_p closer to F_{max} but decreases overall ductility. If plastic fastener deformation is relied upon for ductility in a PDE connection, the use of high strength steel is not recommended.

2.5.3. The issue with pre-loading – Discussion

EN 26891 [52] suggests pre-loading of connections to 40% of the estimated capacity $F_{pre} = 0.4\ F_{max}$. The purpose of pre-loading is to simulate in-situ conditions where the connection has settled (some gravity load present) and to remove initial slip. There are two issues with this approach: a) the capacity may not be known, especially for novel types of connection and b) for soft connections the chosen pre-load may be too high and thus exceeds the linear elastic region. If pre-loading is

chosen to better simulate in-situ conditions, a better pre-load may be $F_{pre} = 0.2 F_{max}$ or $F_{pre} = 0.25 F_y$, and the authors encourage discussion of an appropriate pre-load.

2.6. Brittle connection capacity – state-of-the-art

As previously discussed, the capacity hierarchy needs to be guaranteed by giving explicit, slightly conservative capacity estimates for brittle failure modes. A brittle capacity prediction F_{BR} should be simple and intuitive to avoid errors. Moreover, both ductile and brittle strength predictions need to be sufficiently accurate not only for structural efficiency purposes but more importantly to correctly predict the connection response [67,68].

Quenneville and Morris [69] first presented an intuitive and simple method to estimate the brittle capacity of bolted and dowelled connections based on failure planes and differences in stiffness between head tensile and shear planes.

Cabrero and Yurrita [70], Cabrero et al. [71], and Yurrita and Cabrero [72–74] reviewed existing brittle failure models and further refined the formulas by Quenneville and Morris [69] for steel-to-timber connections with one or more internal or external steel plates, as well as multiple or single row connections. The method also aims to reflect the non-uniform load distribution in splitting and the potential importance of the end distance [72,74].

However, the method does not currently reflect the reduction of shear planes due to dowel embedment once plastic deformations occur. As a consequence, mode cross-over from ductile response to premature brittle failure may occur [49,53,75]. These mixed failure modes were also described by Zarnani and Quenneville [76] and confirmed in tests for plug shear failure [67] and considered in a respective model [77]. However, a more generalized consideration of mixed ductile and brittle failure modes is still missing.

2.6.1. Brittle capacity reduction due to embedment

With increasing embedment of the fasteners at larger joint deformations, the effective shear plane lengths relevant for brittle failure modes, such as block shear and row shear failure, decrease. Fig. 9 illustrates the decrease of brittle capacity due to fastener embedment for a connection loaded parallel to the grain. Mode cross-over occurs when the brittle capacity curve intersects with the ductile load–displacement curve [49,53,75].

As previously discussed, the target plastic displacement is already known from the required ultimate displacement Δ_{Fu} and permissible elastic displacement Δ_{el} as $\Delta_{pl} = \Delta_{Fu} - \Delta_{el}$. The reduced brittle capacity $F_{BR,red}$ can thus be calculated by decreasing the shear plane lengths in the brittle capacity calculation.

The proposed simplified method assumes that the plastic displacement Δ_{pl} is constituted entirely of fastener embedment and that all
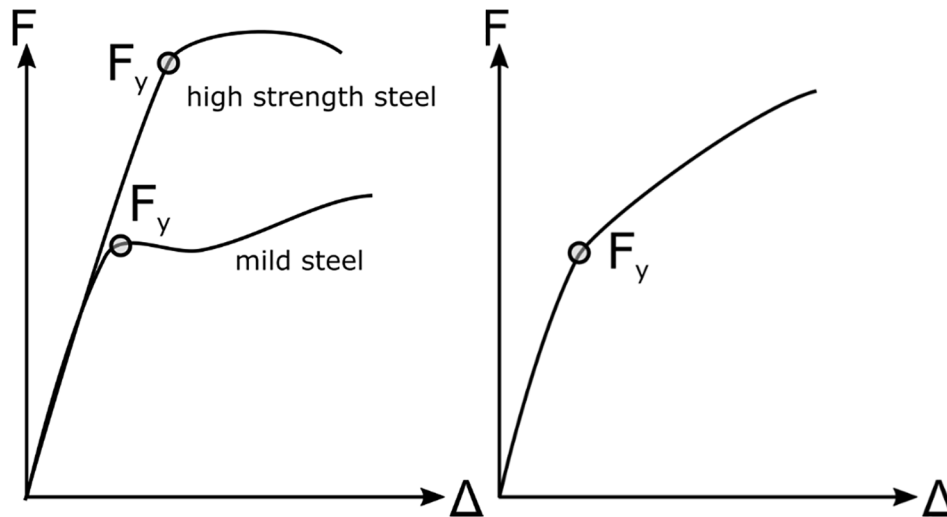

Fig. 8. Tensile test load–displacement curves of mild steel and high strength steel fasteners (left) and load–displacement curve from three-point bending of fastener (right).
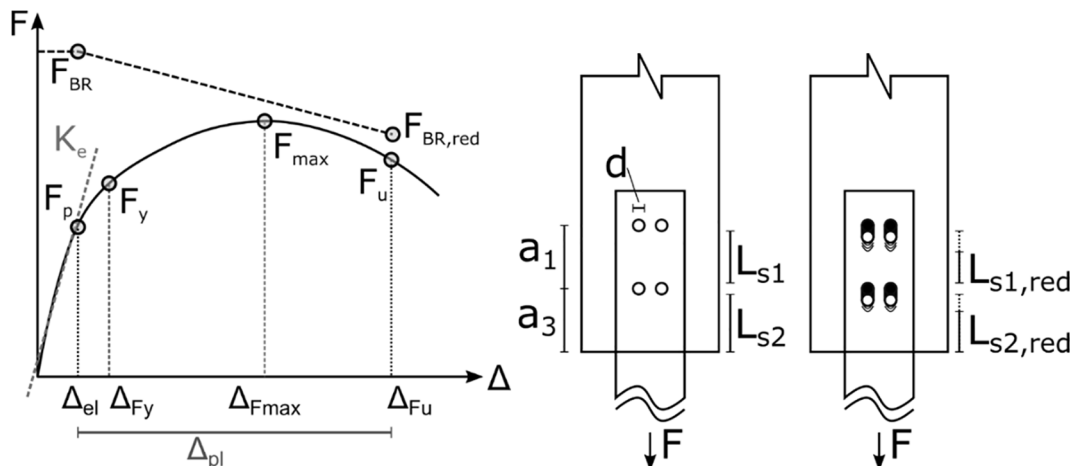

Fig. 9. Reduced brittle capacity: load–displacement curves (left) and shear planes (right).

fasteners exhibit similar embedment once plasticised. The plastic displacement Δ_{pl} is then deducted from fastener spacings and end distance, resulting in a reduced shear plane length $L_{s,red} = (n_1 - 1)(a_1 - d - \Delta_{pl}) + (a_3 - d/2 - \Delta_{pl})$, where n_1 is the number of fasteners parallel to the grain, a_1 is the fastener spacing parallel to the grain, a_3 is the end distance, and d is either the fastener or hole diameter, whichever is larger.

For a bolted or dowelled PDE connection with rigid fasteners that activate the full member thickness t the reduced row shear capacity is $F_{RS,red} = f_s\, 2\, n_2\, L_{s,red}$ and reduced group tear-out capacity $F_{GT,red} = K_s f_s\, 2\, t\, L_{s,red} + K_t f_t\, t\,(n_2 - 1)(a_2 - d)$, where n_2 is the number of rows of fasteners, a_2 is the fastener spacing perpendicular to the grain, K_s and K_t designate the shear plane and head plane stiffness, and f_s and f_t are the shear and tensile strength respectively. The net tensile capacity F_{NT} is not affected.

In the draft of the chapter connections for Eurocode 5 the reduced shear length is not considered and the row shear and plug shear capacity of a nailed or screwed connection are defined as follows (adapted notation):

Row shear capacity: $F_{RS} = 2\, n_2\, F_{s,l}$, with $F_{s,l} = K_s\, t_{ef}\, L_s\, f_s$ and $K_s = 0.4 + 1.4\, \sqrt{(G_{mean} / E_{0,mean})}$, where G_{mean} is the mean shear modulus and $E_{0,mean}$ is the Young's modulus parallel to the grain, and $L_s = (n_1 - 1)\, a_1 + a_3$. The effective thickness t_{ef} depends on the ductile response (EYM mode) and location of plastic hinges, with $t_{ef} = t$ for rigid fasteners.

Plug shear failure: $F_{PS} = max\{2\, F_{s,l}, (F_t + F_b)\}$ where $F_{s,l}$ is the side shear plane, $F_t = K_t f_t\, b_{net}$ is the head tensile capacity with $K_t = 0.9 + 1.4 \sqrt{(G_{mean} / E_{0,mean})}$ and $b_{net} = (n_2 - 1)(a_2 - d)$, and $F_b = K_s L_s b_{net} f_s$ is the bottom shear plane capacity.

Detailed explanations of these approaches are given in Yurrita and Cabrero [72–74] for row shear and block shear, Yurrita and Cabrero [74] for splitting, Yurrita et al. [77] for plug shear, and Yurrita and Cabrero [72–74] for the consideration of uneven load distribution along the fasteners by means of effective thickness.

2.6.2. Possible mode cross-over due to hardening

As previously established, overstrength of the ductile response poses a threat to the capacity hierarchy and needs to be quantified. However, overstrength may further increase with deformation due to timber densification as a result of embedment crushing and steel strain hardening as shown in Fig. 10. This effect yet remains to be quantified.

2.6.3. Load distribution between fasteners

Blaß [78] stipulated that the outer fasteners experience the highest load in a connection. Other simplified analytical models assume a linear load distribution between fasteners in a row (parallel-to-grain loading), where the load on a fastener increases proportionally with the distance from the loaded end. At the onset of yield in the connection assembly, the highest loaded fasteners start to develop plastic hinges which leads to load redistribution. At the ultimate point F_u, there will be more yielding (of the steel) and crushing (of the timber) at the fasteners
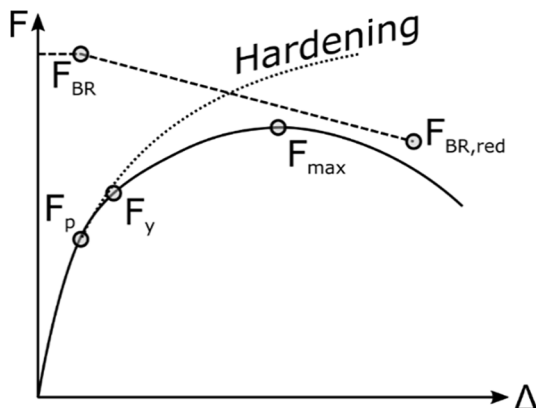

Fig. 10. Capacity increase due to hardening.

farthest from the end; however, brittle tensile failure of the connection assembly is also more likely to be initiated at these fasteners. The effect of non-linear load distributions between fasteners on the ductile strength has since been explored [79] and is currently reflected by n_{ef} in Eurocode 5 [80]. However, the current use n_{ef} of penalises connections with a large number of fasteners and may even lead to brittle failure through artificial reduction of the ductile capacity, which may falsely suggest that ductile response is governing when it is not [67,68].

Yurrita and Cabrero [74] studied the splitting capacity of connections, based on connection length and effective thickness, taking into account the effect of the non-uniform load distribution along a fastener in the timber. However, the exact effect of load distribution between fasteners on brittle capacities and ductility or maximum achievable Δ_{Fu} remains to be quantified. It has been established that connections with more rows of fasteners are more ductile than connections with more fasteners in longer rows, but it is not certain whether this is due to the non-uniform load distribution between fasteners or since the capacity hierarchy was not maintained.

The authors believe that further research is needed to capture the impact of load distribution on brittle capacity and connection ductility.

2.6.4. Brittle failure of CLT

CLT can fail in a brittle manner as reported by e.g. Zarnani and Quenneville [81,82], Ottenhaus et al. [35,48], or Tuhkanen and Ojamaa [83], and the failure modes are complex. The glue bond strength between layers needs to be verified to avoid delamination and opening up of the panels. In addition, bolts with large washers or external steel plate in the end-row may also be advisable. Corner connections are especially critical and reinforcement may be necessary. Simplified models to predict brittle failure urgently need to be developed.

2.7. Robustness and reliability – importance of ductility

Different material and geometrical parameters of the fasteners and the connection influence the response, failure mode, and failure behaviour [12,84]. A connection response with plastic hinging of the metal fasteners generally results not only a higher ductility, but also a lower variability [12]. This lower variability requires a lower partial safety factor for the respective response / failure mode, which is accounted for in Eurocode 5 by an increase of 15% for the EYM modes with two plastic hinges. In addition, not only is the variability smaller but the test results are also observed to be higher than the predictions according to EYM [85].

In contrast, the EYM modes that predominantly result in fastener embedment and little plastic hinging show a large variability and require higher partial safety factors. In particular, the failure of multiple fastener connections is governed by splitting and fracture, as discussed above. The lack of adequate design approaches for these brittle failure modes in design standards poses an additional problem to engineers, since relevant failure modes in the design may not be identified, despite "formally" fulfilling all requirements defined in a design standard [86]. If experience, based on a thorough understanding of these failure phenomena is not able to compensate for some of this uncertainty, then higher safety factors need to be specified. This includes the specification of minimum spacing and distances, that ensure a sufficiently low probability of brittle failure to occur as discussed in Cabrero et al. [71].

From a robustness perspective, it is not sufficient to aim to achieve similar low probabilities of failure for brittle and ductile failure modes, as is currently the case in Eurocode 5, where the same partial factors are applied for different failure modes [80]. Instead, the consequences of different types of failure behaviour should be considered in combination with probability of occurrence to fully capture risk and hence define requirements for robustness.

The robustness can be evaluated on different levels of scale, as discussed by Voulpiotis et al. [87].

1) On a connection scale, brittle failure modes do not allow for a redistribution of forces in a connection and can lead to progressive failure especially for multiple fastener connections [12]. Hence, connections might fail before reaching the desired load-carrying capacity. At the present time, this is partly compensated by considering the effective number of fasteners [24]; however, this blurs the occurrence of brittle failure modes when designing according to the EYM. This is especially true for cases where the effective number of fasteners is much smaller than the actual number of fasteners. This situation should be avoided, not only due to the risk of occurrence of associated brittle failure modes, but also with regard to efficiency of the connection.

2) On a structural scale, the ductility requirements on connections are imposed from the need to accommodate rotations and displacements after a member (wall, column) has failed. Under sustaining or even increased load, the connection redistributes loads within the structure and prevents progressive collapse. The target displacement Δ_T (or rotation θ_T) can be calculated from the changed geometry, and validated through tests, as demonstrated by Mpidi Bita and Tannert [88], Cheng et al. [89] or Lyu et al. [90].

3. Summary and conclusions

This paper discussed current issues in the design of connections that serve as potential ductile elements (PDEs), highlighted areas in need of further research, and suggested design principles to achieve adequate ductile behaviour. The purpose of ductility is to give sufficient warning in case of overloading and to accommodate displacements.

The ideal load–displacement curve for a PDE connection depicted in Fig. 11 can be described by a linear elastic part up until the proportional limit F_p with elastic displacement Δ_{el}, a non-linear softening and plasticisation part that is caused by a combination of timber embedment and fastener yielding, up until the maximum load capacity / peak force F_{max} is reached with respective displacement Δ_{Fmax}, and a softening region until the ultimate capacity F_u and ultimate displacement Δ_{Fu} are reached. The total plastic deformation is $\Delta_{pl} = \Delta_{Fu} - \Delta_{el}$. Brittle failure is not permissible up until Δ_{Fu} which needs to meet or exceed the target displacement Δ_T. The PDE connection needs to accommodate this displacement without significant strength loss.

The yield point F_y is located between F_p and F_{max} and can be a suitable design point for low-damage systems and those systems requiring a capacity reserve.

The brittle capacity of the connection itself and connected members needs to exceed the peak capacity and connection overstrength
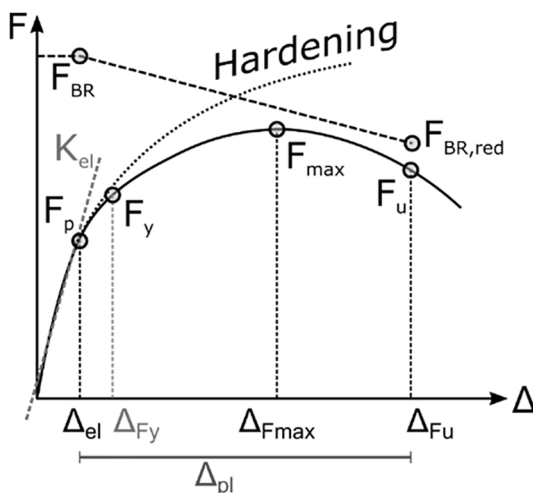
(capacity hierarchy); however, brittle capacity decreases after onset of yielding due to reduction of effective shear plane lengths. Furthermore, additional ovesrstrength due to strain hardening of the fasteners and embedment densification needs to be considered.

3.1. Key Recommendations

The suggested approach is neither displacement based nor force based, but rather specifies required performance targets. (The following recommendations refer to forces "F" and displacements "Δ" but are equally applicable to moments "M" and rotations "θ").

- **Limitation of elastic deformations:** a maximum elastic displacement Δ_{el} may be defined depending on the desired elastic response (soft or rigid / stiff).
  - $\rightarrow$ Guarantees sufficient elastic stiffness K_{el} (wind or gravity serviceability limit state) and limits accelerations under wind / seismic / vibration loads.
- **Accommodation of target displacement:** the target displacement can be derived from the overall structural response and can e.g. be calculated from permissible drift limits. The PDE connection needs to be able to accommodate this target displacement without significant strength loss at its ultimate point (F_u, Δ_{Fu}) with $F_u = 0.8\ F_{max}$. The plastic displacement is $\Delta_{pl} = \Delta_{Fu} - \Delta_{el}$. This requires connection and assembly tests of PDEs to be continued until a strength loss of 20% has occurred; i.e. they should not be prematurely terminated at a slip of 15 mm or 30 mm for monotonic of cyclic loading, respectively. Furthermore, connection manufacturers should provide relevant displacement values (Δ_{el}, Δ_{Fmax}, Δ_{Fu}) to enable designers to select connections with adequate ductility for the intended purpose.
- **Definition of target capacity:** the target capacity can be either the peak capacity F_{max} or yield capacity F_y depending on whether a low-damage design is required.
  - $\rightarrow$ **The yield point (F_y, Δ_{Fy})** is a suitable design point for low-damage design of structures, force-governed loading scenarios (e.g. snow), structures that require a capacity reserve of 20–30%, and may be appropriate for serviceability limit state. The yield point is also suited as design point for loading scenarios that involve reverse-cyclic loading / vibrations that are susceptible to low cycle fatigue.
    The yield capacity F_y can be estimated using the European Yield Model (EYM) with an effective embedment strength $f_{h,e} = 0.8\ f_h$ and yield moment $M_{el} = f_y\ \pi\ d^3/32$ and is often 70–80% of F_{max}. The yield displacement Δ_y is generally close to Δ_{el} and it is usually not necessary to determine Δ_y.
  - $\rightarrow$ **The peak point (F_{max}, Δ_{Fmax})** should be calculated with the plastic moment $M_{pl} = f_y\ d^3/6$ and is a suitable design point for life-safety of displacement governed loading scenarios (wind or seismic ultimate limit state). If the peak point is selected as design point, sufficient post-peak displacement-ability is required with $\Delta_{Fu} - \Delta_{Fmax} \geq 1/3\ \Delta_{pl}$.
- **Guarantee capacity hierarchy:** the brittle capacity F_{BR} needs to be well defined, and needs to consider different failure modes, the effect of connection deformation and non-linearity; e.g. by quantifying the reduction of shear plane lengths due to embedment deformation which yields a reduced brittle capacity $F_{BR,red}$.
  - $\rightarrow$ $F_{BR,red}$ can be calculated by deducting Δ_{pl} from shear plane lengths.
  - $\rightarrow$ Brittle failure / mode cross-over is not permissible up until Δ_{Fu}.
  - $\rightarrow$ Connection overstrength needs to be taken into account $F_{BR,red,d} \geq \gamma_{Rd}\ F_{max,d}$, including overstrength from embedment densification and strain hardening. Overstrength should be limited where possible and not be relied upon as a capacity reserve. If a capacity reserve is required, it is better to pick the yield point as design point.

Fig. 11. Ideal load–displacement curve for PDE connections, including brittle capacity requirements and potential overstrength from hardening effects.

The above recommendations should be seen as one possible approach to achieve truly ductile connection response without premature brittle failure. In doing so, several issues have been raised that require further clarification. Finally, the authors hope to stimulate further discussion of these issues especially in the context of design codes.

Declaration of Competing Interest

The authors declare that they have no known competing financial interests or personal relationships that could have appeared to influence the work reported in this paper.

References

[1] T.E. McLain, Connectors and fasteners: Research Needs and Goals, in: K.J. Fridley (Ed.), Wood Engineering in the 21st Century, ASCE, Reston, VA, 1998, pp. 56–69.

[2] T. Smith, D. Moroder, F. Sarti, Stefano Pampanin, A.H. Buchanan, The reality of seismic engineering in a modern timber world. In Proceedings of INTER Meeting 2015, 2015.

[3] Popovski, M., & Karacabeyli, E. (2005). Framework for Lateral Load Design Provisions for Engineered Wood Structures in Canada. CIB W18, (August), CIB-W18/38-15-3.

[4] Sarti, F., Palermo, A., & Pampanin, S. (2014). Design and Testing of Post-Tensioned Timber Wall Systems. World Conference on Timber Engineering, (August), 2–3.

[5] F. Sarti, A. Palermo, S. Pampanin, Quasi-Static Cyclic Testing of Two-Thirds Scale Unbonded Posttensioned Rocking Dissipative Timber Walls, J. Struct. Eng. 142 (4) (2016) 1–14, https://doi.org/10.1061/(asce)st.1943-541x.0001291.

[6] A. Hashemi, P. Zarnani, R. Masoudnia, P. Quenneville, Experimental Testing of Rocking Cross-Laminated Timber Walls with Resilient Slip Friction Joints, J. Struct. Eng. 144 (1) (2018) 04017180, https://doi.org/10.1061/(asce)st.1943-541x.0001931.

[7] H. Rainer, E. Karacabeyli, Wood-Frame Construction Meeting the Challenges of Earthquakes. In Building Performance Series, 2003.

[8] J.M. Cabrero, B. Iraola, M. Yurrita, in: Handbook of Materials Failure Analysis, Elsevier, 2018, pp. 123–152, https://doi.org/10.1016/B978-0-08-101928-3.00007-0.

[9] E. Frühwald Hansson, Analysis of structural failures in timber structures: Typical causes for failure and failure modes, Eng. Struct. 33 (11) (2011) 2978–2982, https://doi.org/10.1016/j.engstruct.2011.02.045.

[10] Köhler, J., Fink, G., & Toratti, T. (2011). Assessment of failures and malfunctions, Publication of COST Action E55-Modelling of the performance of timber structures.

[11] A. Jorissen, M. Fragiacomo, General notes on ductility in timber structures, Eng. Struct. 33 (11) (2011) 2987–2997, https://doi.org/10.1016/j.engstruct.2011.07.024.

[12] Jockwer, R., G. Fink, and J. Köhler. "Assessment of the Failure Behaviour and Reliability of Timber Connections with Multiple Dowel-Type Fasteners." Engineering Structures 172 (October 1, 2018): 76–84. https://doi.org/10.1016/j.engstruct.2018.05.081.

[13] F. Brühl, U. Kuhlmann, A. Jorissen, Consideration of plasticity within the design of timber structures due to connection ductility, Eng. Struct. 33 (11) (2011) 3007–3017, https://doi.org/10.1016/j.engstruct.2011.08.013.

[14] A.H. Buchanan, The challenges for designers of tall timber buildings. WCTE 2016 - World Conference on Timber Engineering, 2016.

[15] D. Trutalli, L. Marchi, R. Scotta, L. Pozza, Capacity design of traditional and innovative ductile connections for earthquake-resistant CLT structures, Bull. Earthq. Eng. 17 (4) (2019) 2115–2136, https://doi.org/10.1007/s10518-018-00536-6.

[16] D. Casagrande, S. Bezzi, G. D'Arenzo, S. Schwendner, A. Polastri, W. Seim, M. Piazza, A methodology to determine the seismic low-cycle fatigue strength of timber connections, Constr. Build. Mater. 231 (2020) 117026, https://doi.org/10.1016/j.conbuildmat.2019.117026.

[17] M. Izzi, A. Polastri, Low cycle ductile performance of screws used in timber structures, Constr. Build. Mater. 217 (2019) 416–426, https://doi.org/10.1016/j.conbuildmat.2019.05.087.

[18] Maurizio Piazza, Andrea Polastri, Roberto Tomasi, Ductility of timber joints under static and cyclic loads, Proceedings of the Institution of Civil Engineers-Structures and Buildings 164 (2) (2011) 79–90.

[19] G.N. Boughton, K. Crews, Timber design handbook: in accordance with the Australian Limit State Timber Design Code AS 1720.1-2010: timber structures, Standards Australia, Sydney NSW, 2013.

[20] Pei, S., Lindt, J. Van De, Barbosa, A., Berman, J., Dolan, J., Zimmerman, R. B., … Ryan, K. (2018). Full-Scale Shake Table Test of Mass-Timber Building With Resilient Post-Tensioned Rocking Walls. World Conference on Timber Engineering, 8–13.

[21] H.-E. Blomgren, S. Pei, Z. Jin, J. Powers, J.D. Dolan, J.W. van de Lindt, A. R. Barbosa, D. Huang, Full-Scale Shake Table Testing of Cross-Laminated Timber Rocking Shear Walls with Replaceable Components, J. Struct. Eng. 145 (10) (2019) 04019115, https://doi.org/10.1061/(ASCE)ST.1943-541X.0002388.

[22] Cabrero, J.M., Stepinac, M., Ranasinghe, K., & Kleiber, M. (2018). Results from a questionnaire for practitioners about the connections chapter of Eurocode 5.

Sandhaas, C., Munch-Andersen, J., & Dietsch, P. (Eds.). Design of Connections in Timber Structures.

[23] Blaß H.J., Biehnhaus A., Krämer V. (2000): Effective bending capacity of dowel-type fasteners. In: Proc. of the CIB-W18 Meeting 33, Delft, The Netherlands, Paper No. CIB-W18/33-7-5.

[24] A. Jorissen, Double shear timber connections with dowel type fasteners, PhD thesis, Technische Universiteit Delft, Delft, The Netherlands, 1998.

[25] Follesa, M., Fragiacomo, M., Casagrande, D., Tomasi, R., Piazza, M., Vassallo, D., & Rossi, S. (2016). The new version of chapter 8 of Eurocode 8. WCTE 2016 - World Conference on Timber Engineering.

[26] Follesa, M., Fragiacomo, M., Casagrande, D., Tomasi, R., Piazza, M., Vassallo, D., … Rossi, S. (2018). The new provisions for the seismic design of timber buildings in Europe. Engineering Structures, 168(December 2017), 736–747. https://doi.org/10.1016/j.engstruct.2018.04.090.

[27] AS 1720.1-2010 (2010). Timber structures Part 1 : Design methods. Standards Australia Limited, GPO Box 476, Sydney, NSW 2001, Australia. ISBN 978 0 7337 9429 2.

[28] I. Smith, G.C. Foliente, M. Syme, R. McNamara, C. Seath, Development of Limit States Design Method for Timber Joints with Dowel Type Fasteners Part 2 Comparison of Experimental Results with European Yield Model (EYM) Predictions, Forest & Wood Products Research & Development Corporation. (2004).

[29] SIA, Standard SIA 265 - Timber Structures, SIA Swiss Society of Engineers and Architects, Zurich, Switzerland, 2012.

[30] R. Park, T. Paulay (Eds.), Reinforced Concrete Structures, Wiley, 1975.

[31] Ottenhaus, L. M., Li, M., & Smith, T. (2020). Analytical Derivation and Experimental Verification of Overstrength Factors of Dowel-type Timber Connections for Capacity Design. Journal of Earthquake Engineering, 00(00), 1–15. https://doi.org/10.1080/13632469.2020.1781711.

[32] J.R. Brown, M. Li, Structural performance of dowelled cross-laminated timber hold-down connections with increased row spacing and end distance, Constr. Build. Mater. 271 (2020) 121595, https://doi.org/10.1016/j.conbuildmat.2020.121595.

[33] Stehn L, Björnfot A. (2002). Comparison of different ductility measurements for a nailed steel-to-timber connection. In: Proceedings of the 7th world conference on timber engineering WCTE 2002.

[34] Flatscher, G. (2017). Evaluation and approximation of timber connection properties for displacement-based analysis of CLT wall systems. PhD Thesis. TU Graz.

[35] Ottenhaus, L.-M. (2019). Seismic Performance of Dowel-Type Connections in Tall Timber Buildings. PhD Thesis. University of Canterbury.

[36] Jockwer, R., and A. Jorissen. 2018. 'Load-Deformation Behaviour and Stiffness of Lateral Connections with Multiple Dowel Type Fasteners'. In Proc. of the INTER Meeting 51, 51-7–7. Tallinn, Estonia: Timber Scientific Publishing, Karlsruhe, Germany.

[37] Smith, I., Asiz, A., Snow, M., & Chui, Y. H. (2006). Possible Canadian / ISO Approach to Deriving Design Values From Test Data. CIB W18 Meeting, (39).

[38] Muñoz W, Mohammad M, Salenikovich A, Quenneville P. (2008). Need for a harmonized approach for calculations of ductility of timber assemblies. In: Proceedings of the meeting 41 of the working commission W18-timber structures. CIB. 2008.

[39] Karacabeyli E, Ceccotti A. Nailed wood-frame shear walls for seismic loads: Test results and design considerations. Struct Eng World Wide 1998; Paper ref. T207-6.

[40] Yasumura M, Kawai N. (1998). Estimating seismic performance of wood-framed structures. In: Proceedings of 1998 IWEC Switzerland. vol. 2. p. 564–71.

[41] Howtec, Allowable Stress Calculation for Conventional Beam and Post Housing, Japan Housing and Wood Technology Center (HOWTEC), Tokyo, Japan, 2017.

[42] Foliente G. C. (1996) Issues in seismic performance testing and evaluation of timber structural systems. In: Proceedings of the 1996 international timber engineering conference. vol. 1. p. 1.29–.36.

[43] ASTM D5764-97a. (2013). Standard Test Method for Evaluating Dowel-Bearing Strength of Wood and Wood-Based Products. https://doi.org/10.1520/D5764-97AR13.2.

[44] EN 12512:2001, Timber structures, Test methods. Cyclic testing of joints made with mechanical fasteners, European Committee for Standardization, Brussels, 2001.

[45] M. Schweigler, T.K. Bader, G. Hochreiner, R. Lemaître, Parameterization equations for the nonlinear connection slip applied to the anisotropic embedment behavior of wood, Compos. B Eng. 142 (2018) 142–158, https://doi.org/10.1016/j.compositesb.2018.01.003.

[46] Schweigler, M., Bader, T. K., Bocquet, J. F., Lemaître, R., & Sandhaas, C. (2019). Embedment test analysis and data in the context of phenomenological modeling for dowelled timber joint design. International Network on Timber Engineering Research (INTER) - Meeting Fifty-Two, Tacoma (US), INTER / 52-07-8, 1–17.

[47] G.M. Calvi, M.J.N. Priestley, M.J. Kowalsky, Displacement-Based Seismic Design of Structures, Earthquake Sepctra 24 (2) (2008) 555.

[48] L.M. Ottenhaus, M. Li, T. Smith, Structural performance of large-scale dowelled CLT connections under monotonic and cyclic loading, Eng. Struct. 176 (August) (2018) 41–48, https://doi.org/10.1016/j.engstruct.2018.09.002.

[49] Lisa-Mareike Ottenhaus, Minghao Li, Tobias Smith, Pierre Quenneville, Overstrength of dowelled CLT connections under monotonic and cyclic loading, Bull. Earthq. Eng. 16 (2) (2017) 753–773, https://doi.org/10.1007/s10518-017-0221-8.

[50] Chuang, W. C., & Spence, S. M. J. (2019). An efficient framework for the inelastic performance assessment of structural systems subject to stochastic wind loads.

Engineering Structures, 179(November 2018), 92–105. https://doi.org/10.1016/j.engstruct.2018.10.039.

[51] W.C. Chuang, S.M.J. Spence, Probabilistic performance assessment of inelastic wind excited structures within the setting of distributed plasticity, Struct. Saf. 84 (January) (2020), 101923, https://doi.org/10.1016/j.strusafe.2020.101923.

[52] EN 26891:1991 (1991). Timber Structures - Joints Made with Mechanical Fasteners - General Principles for the Determination of Strength and Deformation Characteristics. European Committee for Standardization, Brussels.

[53] L.-M. Ottenhaus, M. Li, T. Smith, P. Quenneville, Mode Cross-Over and Ductility of Dowelled LVL and CLT Connections under Monotonic and Cyclic Loading, J. Struct. Eng. 144 (7) (2018) 04018074, https://doi.org/10.1061/(asce)st.1943-541x.0002074.

[54] L.-M. Ottenhaus, M. Li, T. Smith, P. Quenneville, Ductility of dowelled and nailed CLT and LVL connections under monotonic and cyclic loading. Australian Earthquake Engineering Society 2016 Conference, 2016.

[55] P.D. Rodd, The analysis of timber joints made with circular dowel connectors, PhD Thesis, University of Sussex, 1973.

[56] Johan Sjödin, Erik Serrano, Bertil Enquist, An experimental and numerical study of the effect of friction in single dowel jointsExperimentelle und rechnerische Untersuchung des Einflusses von Reibung in Verbindungen mit einem Stabdübel, Holz Roh Werkst 66 (5) (2008) 363–372.

[57] M. Yurrita, J.M. Cabrero, New criteria for the determination of the parallel-to-grain embedment strength of wood, Constr. Build. Mater. 173 (2018) 238–250, https://doi.org/10.1016/j.conbuildmat.2018.03.127.

[58] G.W. Trayer, The bearing strength of wood under bolts Vol. 326 (1932) 1932.

[59] AS/NZS ISO 10984.2:2015. (2015). Timber structures—Dowel-type fasteners Part 2: Determination of embedding strength. Jointly published by SAI Global Limited under licence from Standards Australia Limited, GPO Box 476, Sydney, NSW 2001 and by Standards New Zealand, Private Bag 2439, Wellington 6140.

[60] EN 383:2007, Timber structures - Test methods - Determination of embedment strength and foundation values for dowel type fasteners, European Committee for Standardization, Brussels, 2007.

[61] S. Franke, N. Magnière, Discussion of testing and evaluation methods for the embedment behaviour of connections. International Network on Timber Engineering Research (INTER), 2014.

[62] E. Tuhkanen, J. Mölder, G. Schickhofer, Influence of number of layers on embedment strength of dowel-type connections for glulam and cross-laminated timber, Eng. Struct. 176(September) (2018) 361–368, https://doi.org/10.1016/j.engstruct.2018.09.005.

[63] L.-M. Ottenhaus, M. Li, Embedment Strength of New Zealand Cross Laminated Timber, New Zealand Timber Design Journal 26 (1) (2018) 12–16.

[64] H.J. Blaß, A. Bienhaus, V. Krämer, Effective bending capacity of dowel-type fasteners, Proceedings of the International RILEM Symposium Joints in Timber Structures, Stuttgart 22 (2001) 71–88.

[65] H.J. Blass, F. Colling, Load-carrying capacity of dowelled connections, International Network on Timber Engineering Research, INTER / (2015) 48-7-3.

[66] AS/NZS ISO 10984.1:2015. (2015). Timber structures—Dowel-type fasteners Part 1: Determination of yield moment. Jointly published by SAI Global Limited under licence from Standards Australia Limited, GPO Box 476, Sydney, NSW 2001 and by Standards New Zealand, Private Bag 2439, Wellington 6140.

[67] Miguel Yurrita, José Manuel Cabrero, Experimental Analysis of Plug Shear Failure in Timber Connections with Small Diameter Fasteners Loaded Parallel-to-Grain, Eng. Struct. 238 (2021) 111766, https://doi.org/10.1016/j.engstruct.2020.111766.

[68] Miguel Yurrita, José Manuel Cabrero, On the need of distinguishing ductile and brittle failure modes in timber connections with dowel-type fasteners, Eng. Struct. 242 (2021) 112496, https://doi.org/10.1016/j.engstruct.2021.112496.

[69] P. Quenneville, H. Morris, Proposal for a mechanics-based bolted connection design approach for AS1720.1, Aust. J. Struct. Eng. 9 (3) (2009) 195–206, https://doi.org/10.1080/13287982.2009.11465022.

[70] Cabrero, J. M., & Yurrita, M. (2018). Performance assessment of existing models to predict brittle failure modes of steel-to-timber connections loaded parallel-to-grain with dowel-type fasteners. Engineering Structures, 171(November 2017), 895–910. https://doi.org/10.1016/j.engstruct.2018.03.037.

[71] J.M. Cabrero, D. Honfi, R. Jockwer, M. Yurrita, A probabilistic study of brittle failure in dowel-type timber connections with steel plates loaded parallel to the grain, Wood Mat. Sci. Eng. 14 (5) (2019) 298–311, https://doi.org/10.1080/17480272.2019.1645206.

[72] Yurrita, M., & Cabrero, J. M. (2020b). Effective thickness of timber elements for the evaluation of brittle failure in timber-to-steel connections with large diameter fasteners loaded parallel-to-grain at the elastic range: A new method based on a beam on elastic foundation. Engineering Structures, 209(December 2019), 109959. https://doi.org/10.1016/j.engstruct.2019.109959.

[73] M. Yurrita, J.M. Cabrero, New design model for brittle failure in the parallel-to-grain direction of timber connections with large diameter fasteners, Eng. Struct. 217 (June) (2020), 111155, https://doi.org/10.1016/j.engstruct.2020.110557.

[74] M. Yurrita, J.M. Cabrero, New design model for splitting in timber connections with one row of fasteners loaded in the parallel-to-grain direction, Eng. Struct. 223 (February) (2020), 111155, https://doi.org/10.1016/j.engstruct.2020.111155.

[75] Novis, S. A. L., Jacks, J., & Quenneville, P. (2016). Predicting the Resistance and Displacement of Timber Bolted Connections. WCTE 2016 - World Conference on Timber Engineering.

[76] P. Zarnani, P. Quenneville, Strength of Timber Connections under Potential Failure Modes: An Improved Design Procedure, Constr. Build. Mater. 60 (2014) 81–90, https://doi.org/10.1016/j.conbuildmat.2014.02.049.

[77] Miguel Yurrita, José Manuel Cabrero, Ezequiel Moreno-Zapata, Brittle Failure in the Parallel-to-Grain Direction of Timber Connections with Small Diameter Dowel-Type Fasteners: A New Design Model for Plug Shear, Eng. Struct. 241 (2021) 112450, https://doi.org/10.1016/j.engstruct.2021.112450.

[78] Blaß H. (1990) Load distribution in nailed joints, in: CIB-W18 Timber structures, Lisbon, Portugal, Paper 23–7–2; 1990.

[79] Bader, T. K., Bocquet, J.-F., Schweigler, M., Lemaitra, R. (2018) Numerical modeling of the load distribution in multiple fastener connections. Sandhaas, C., Munch-Andersen, J., & Dietsch, P. (Eds.). Design of Connections in Timber Structures.

[80] EN 1995-1-1:2004/2008. (2004). Eurocode 5: Design of timber structures — Part 1-1: General — Common rules and rules for buildings. https://doi.org/10.1680/cien.2001.144.6.39.

[81] P. Zarnani, P.J.H. Quenneville, Resistance of Connections in Cross-Laminated Timber (CLT) Under Block Tear-Out Failure Mode. International Network on Timber Engineering Research (INTER), 2014.

[82] P. Zarnani, P. Quenneville, New design approach for controlling brittle failure modes of small-dowel-type connections in Cross-laminated Timber (CLT), Constr. Build. Mater. 100 (2015) 172–182, https://doi.org/10.1016/j.conbuildmat.2015.09.049.

[83] E. Tuhkanen, M. Ojamaa, Early experimental investigations on slotted-in steel plate connections with self-perforating dowels in CLT, Wood Mat. Sci. Eng. 16 (2) (2021) 102–109, https://doi.org/10.1080/17480272.2019.1626482.

[84] Jockwer, R. "Impact of Varying Material Properties and Geometrical Parameters on the Reliability of Shear Connections with Dowel Type Fasteners." In Proc. of the INTER Meeting 3/Paper 49-7-1. Graz, Austria, 2016.

[85] J. Köhler, Reliability of timber structures, Swiss Federal Institute of Technology, DISS, ETH NO, 2006, p. 16378.

[86] Ranasinghe, K., Cabrero, J. M., Stepinac, M., & Kleiber, M. (2018). Practitioners' Opinions About the En 1995 – Results From Comprehensive Online Survey. World Conference in Timber Engineering 2018.

[87] Konstantinos Voulpiotis, Jochen Köhler, Robert Jockwer, Andrea Frangi, A holistic framework for designing for structural robustness in tall timber buildings, Eng. Struct. 227 (2021) 111432, https://doi.org/10.1016/j.engstruct.2020.111432.

[88] Hercend Mpidi Bita, Thomas Tannert, Experimental Study of Disproportionate Collapse Prevention Mechanisms for Mass-Timber Floor Systems, J. Struct. Eng. 146 (2) (2020) 04019199, https://doi.org/10.1061/(ASCE)ST.1943-541X.0002485.

[89] Cheng, X., Gilbert, B. P., Guan, H., Underhill, I. D., & Karampour, H. (2021). Experimental dynamic collapse response of post-and-beam mass timber frames under a sudden column removal scenario. Engineering Structures, 233(June 2020), 111918. https://doi.org/10.1016/j.engstruct.2021.111918.

[90] Lyu, C. H., Gilbert, B. P., Guan, H., Underhill, I. D., Gunalan, S., & Karampour, H. (2021). Experimental study on the quasi-static progressive collapse response of post-and-beam mass timber buildings under an edge column removal scenario. Engineering Structures, 228(October 2020), 111425. https://doi.org/10.1016/j.engstruct.2020.111425.